Available online at www.sciencedirect.com
ScienceDirect
Journal of Microbiological Methods 67 (2006) 424–436
Journal of Microbiological Methods
www.elsevier.com/locate/jmicmeth

Comparison of aerobic and photosynthetic *Rhodobacter sphaeroides* 2.4.1 proteomes

Stephen J. Callister [a], Carrie D. Nicora [a], Xiaohua Zeng [b], Jung Hyeob Roh [b], Miguel A. Dominguez [c], Christine L. Tavano [d], Matthew E. Monroe [a], Samuel Kaplan [b], Timothy J. Donohue [d], Richard D. Smith [a], Mary S. Lipton [a,*]

[a] *Biological Separations and Mass Spectrometry, Mail Stop: K8-98, Pacific Northwest National Laboratory, Richland WA, 99352, USA*
[b] *Department of Microbiology and Molecular Genetics, University of Texas Health Science Center, Houston TX, 77030, USA*
[c] *Department of Genetics, University of Wisconsin-Madison, Madison WI, 53706, USA*
[d] *Department of Bacteriology, University of Wisconsin-Madison, Madison WI, 53706, USA*

Received 1 April 2006; received in revised form 13 April 2006; accepted 13 April 2006
Available online 7 July 2006

Abstract

The analysis of proteomes from aerobic and photosynthetic *Rhodobacter sphaeroides* 2.4.1 cell cultures by liquid chromatography-mass spectrometry yielded approximately 6,500 high confidence peptides representing 1,675 gene products (39% of the predicted proteins). The identified proteins corresponded primarily to open reading frames (ORFs) contained within the two chromosomal elements of this bacterium, but a significant number were also observed from ORFs associated with 5 naturally occurring plasmids. Using the accurate mass and time (AMT) tag approach, comparative studies showed that a number of proteins were uniquely detected within the photosynthetic cell culture. The estimated abundances of proteins observed in both aerobic respiratory and photosynthetic grown cultures were compared to provide insights into bioenergetic models for both modes of growth. Additional emphasis was placed on gene products annotated as hypothetical to gain information as to their potential roles within these two growth conditions. Where possible, transcriptome and proteome data for *R. sphaeroides* obtained under the same culture conditions were also compared.

Keywords: *Rhodobacter sphaeroides*; Comparative proteomics; Photosynthesis; Fourier transform ion cyclotron resonance mass spectrometry (FTICR MS)

1. Introduction

Rhodobacter sphaeroides is a gram negative purple nonsulfur eubacterium and a member of the α-3 subdivision of the *Proteobacteria* (Woese, 1987; Woese et al., 1984). Within this subgroup, *R. sphaeroides* is a well-studied and free-living microbe that is capable of growth under a variety of conditions, including autotrophic, phototrophic, and anaerobic heterotrophic, using a variety of electron acceptors such as dimethly sulfoxide (DMSO), trimethyl-amine-N48 oxide (TMA) and nitrate to mention a few (Martinezluque et al., 1991; Schultz and Weaver, 1982; Yen and Marrs, 1977). *R. sphaeroides* is known for its diverse abilities including metal

* Corresponding author. Tel.: +1 509 373 9039; fax: +1 509 376 7722.
E-mail address: mary.lipton@pnl.gov (M.S. Lipton).

0167-7012/$ - see front matter © 2006 Elsevier B.V. All rights reserved.
doi:10.1016/j.mimet.2006.04.021

reduction (Nepple et al., 2000; Moore and Kaplan, 1992), nitrogen fixation, and the assimilation of carbon dioxide (Joshi and Tabita, 1996). Additionally, *R. sphaeroides* is capable of producing copious amounts of hydrogen, which could potentially prove to be a source of renewable bioproduced energy (Dubbs and Tabita, 2004; Fang et al., 2005; Moore and Kaplan, 1992). These biochemical processes are linked to *R. sphaeroides*' photosynthetic apparatus that has served as a model for anoxygenic photosynthesis.

Global comparative and functional genomic analyses have been undertaken to discover the existence of additional genes that are either directly or indirectly involved in the photosynthetic lifestyle, beyond the structural and regulatory genes contained within the well characterized photosynthetic gene cluster (PGC) (Zeilstra-Ryalls et al., 1998). These studies have revealed new insights into the role and regulation of mRNA transcripts both outside and within the photosynthetic gene cluster (Choudhary and Kaplan, 2000; Pappas et al., 2004; Roh et al., 2004; Tavano et al., 2005). Herein, we report a global proteomic analysis based on the accurate mass and time (AMT) tag approach (Lipton et al., 2002; Smith et al., 2002). Our objective was to probe the photosynthetic lifestyle of *R. sphaeroides* on a protein level and compare our observations to transcriptome observations either reported in published genomic analyses or made available as supplementary data from microarrays [www.jbc.org/cgi/data/M311608200/DC1/1].

2. Materials and methods

2.1. Culture conditions

Isolated batch cultures of *R. sphaeroides* 2.4.1 (ATCC# BAA-808) were grown in Sistrom's minimal medium (containing succinate) prepared according to established protocols (Cohen-Bazire et al., 1957). To reduce expression of the photosynthetic apparatus during aerobic respiratory growth, batch cultures were sparged with 30% O_2, 69% N_2, and 1% CO_2 using a Linde RM4575 Mass Flowmeter/Flowcontroller (ASGE, Middlesex, NJ). Conversely, cultures were sparged with 95% N_2 and 5% CO_2 under low light intensity (3 W/m^2) to maximize levels of the photosynthetic apparatus. Cell growth was monitored turbidimetrically with a Klett–Summerson colorimeter (Klett Manufacturing Co., New York, NY) equipped with a No. 66 filter. Cells were harvested when cell densities reached $\sim 2 \times 10^8$ cfu/mL to prevent O_2 limitation in the aerobic cultures and to minimize shading of photosynthetic cultures. Cells were placed on ice and then harvested by centrifuging at 5,000 $\times g$ for 20 min at 4 °C. After decanting supernatant, cell pellets were immediately frozen in liquid nitrogen and stored at −80 °C.

2.2. Protein extraction and digestion

Siliconized tubes were used to prepare total (global), insoluble, and soluble protein digests from frozen cultures. For the global protein digest, frozen cells were washed once using 100 mM NH_4HCO_3, pH 8.4 buffer, and then suspended in a new aliquot of this buffer. Cells were lysed by bead beating for 3 min with 0.1 zirconium beads, using a Mini Beadbeater-8 (Biospec Products, Bartlesville, OK) set at maximum speed. Cell lysate was removed by placing the punctured tube containing the lysate and bead suspension into an outer tube, followed by centrifuging at 4 °C and 14 krpm for 5 min. An additional ~200 μl of 100 mM NH_4HCO_3, pH 8.4, was added to the punctured tube and then centrifuged again for an additional 5 min. Proteins within the lysate were denatured and reduced by adding urea and thiourea to a final concentration of 7 M and 2 M, respectively. Fresh dithiothreitol was added to a final concentration of 5 mM, and samples were incubated at 60 °C for 30 min. Following incubation, the global protein sample was diluted 10-fold with 100 mM NH_4HCO_3, pH 8.4, to reduce salt concentration. A volume of 1 M $CaCl_2$ was added to the diluted sample to a final concentration of 1 mM, and the sample was digested at 37 °C using sequencing grade trypsin (Roche, Indianapolis, IN) at a ratio of 1 unit/50 units of protein (1 unit = ~1 μg of protein) for 4 h. Following incubation, digested samples were desalted using an appropriately sized C-18 SPE column (Supelco, St. Louis, MO) and vacuum manifold. Three column volumes of methanol were passed through the column followed by 2 column volumes of nanopure water. After passing the sample through the column, the column was washed with 4 volumes of a 95% acetonitrile (ACN), 0.1% trifluoroacetic acid (TFA) solution. Peptides were eluted using one column volume of an 80% ACN, 0.1% TFA solution. The collected peptides were concentrated to a final volume ranging from 50 μl to 100 μl and measured using the BCA assay (Pierce Chemical Co., Rockfort, IL) according to the manufacturer's instructions.

For the insoluble protein digest, frozen cells were washed once, suspended in 100 mM NH_4HCO_3, pH 7.8, and lysed using bead beating as previously described. The cell lysate was ultracentrifuged at 4 °C and 100 krpm for 10 min. The resulting supernatant that contained soluble proteins was separated from the pellet and retained for digestion as previously described. The pellet was washed by suspension in 100 mM NH_4HCO_3, pH 7.8 using mild

sonication and ultracentrifuged at 100 krpm for 5 min, again at 4 °C. Following centrifugation, the pellet was resuspended in a solubilizing solution that contained 7 M urea, 2 M thiourea, 1% CHAPS in 50 mM NH_4HCO_3, pH 7.8, and an aliquot of 194 mM DTT solution (prepared fresh) that was added to a final sample concentration of 9.7 mM. The insoluble protein sample was incubated and digested as described above with the exception that a 50 mM NH_4HCO_3, pH 7.8 buffer was used for the 10-fold dilution. Following digestion, the pH of the sample was slowly lowered to <4.0 by adding small volumes (1 μl to 2 μl) of 20% formic acid. Removal of salts and detergent was performed using an appropriately sized SCX SPE column (Supelco, St. Louis, MO) and vacuum manifold by first passing three column volumes of methanol through the column. The column was conditioned by a series of rinses (6 column volumes each) using 10 mM ammonium formate in 25% ACN, pH 3.0 (solution 1), 500 mM ammonium formate in 25% ACN, pH 6.8 (solution 2), and nanopure water. After passing the acidified sample through the column, the column was washed with 10 column volumes of solution 1, and peptides were eluted using one column volume of solution 2. Peptides were then concentrated and their concentration measured as described above.

2.3. LC-tandem mass spectrometry and peptide putative mass and elution time tag assignments

Peptides from the global, insoluble, and soluble digests were fractionated (50 to 100 fractions each) using high resolution reversed-phase HPLC (a 65 cm long, 150 μm i.d. × 360 μm o.d. capillary packed with 5 micron particles) (Lipton et al., 2002). The HPLC was operated at 5000 psi with a ~1.8 μl/min flow rate (when equilibrated to 100% mobile phase A). The two mobile phases consisted of 0.2% acetic acid, 0.05% TFA in water (mobile phase A) and 0.1% TFA in 90% ACN and 10% water (mobile phase B). The HPLC was operated in an exponential gradient mode with mobile phase B replacing mobile phase A 10 min after sample injection, which was accomplished by using an in-house mixer, capillary column selector, and sample loop. From each collected fraction, 10 μg (consistent) of peptides were analyzed by this reversed phase HPLC separation coupled ion trap mass spectrometer (LCQ, Thermo Electron, San Jose, CA) that was operated in a data-dependent MS/MS mode. MS/MS spectra were analyzed using the SEQUEST algorithm (Eng et al., 1994) in conjunction with predicted protein annotations obtained from the Joint Genome Institute (JGI; http://www.jgi.doe.gov/). Preliminary filtering of identified peptides was performed using a minimum cross-correlation cut-off (*Xcorr*) of either 1.9, 2.2, or 3.75 for 1+, 2+, or 3+ charge states, respectively, for fully tryptic (peptides that contained either an arginine or lysine at the site of cleavage), partially tryptic, and non-tryptic peptides that were at a minimum, 6 amino acids long. These peptides were further filtered by removing all peptides using a discriminant approach developed at our laboratory (Strittmatter et al., 2004) (based upon a score >0.1). The discriminant score combines 6 SEQUEST parameters with a predicted normalized elution time to assess the quality of the peptide sequence; previous work has shown that peptides with scores <0.1 have a significant false positive identification rate (Strittmatter et al., 2004). Peptides that passed the above filtering criteria were considered as putative mass and elution time (PMT) tags, and placed into a database used in conjunction with subsequent LC-accurate mass measurements. Estimation of percent false positives for the PMT database was calculated by reverse database searching techniques (Qian et al., 2005).

2.4. LC-FTICR MS analyses

Triplicate sub-samples taken from each of the global, soluble, and insoluble protein digests were consecutively analyzed using a capillary LC-FTICR platform (modified 9.4 tesla; Bruker Daltonics) (Belov et al., 2004). LC separations were the same as above but the FTICR mass spectra were acquired with approximately 10^5 resolution, provided low parts per million mass measurement accuracy. The data were analyzed using the ICR-2LS software developed in our laboratory (Smith et al., 2002). Measured masses and normalized elution times of peptides were compared to the previously established PMT tag peptide sequences (Smith et al., 2002). A spatially localized confidence score(Anderson et al., 2004; Norbeck et al., 2005) was calculated for those peptides, targeting multiple amino acid sequences within a mass measurement accuracy of ±6 ppm and normalized LC elution time window of 5% (less than 5% difference between observed elution time and average elution time). Peptides with scores less than 0.75 were more likely to be incorrect (false positive) due to the presence of peptide PMT tags with very similar LC elution times and accurate masses, and were discarded.

2.5. Comparative abundance analysis

Measured arbitrary abundances were determined by integrating the areas under each peak of the LC-FTICR peak for a detected peptide (Smith et al., 2002). Abundances of peptides identified across instrument replicates and cell cultures for each digest (insoluble and soluble)

were aligned using the quantile technique (Bolstad et al., 2003). If a peptide was identified in one sample preparation but not the other (not uncommon for low level species), then half the minimum observed arbitrary abundance from the data set was assigned to that peptide to facilitate visualization and comparison. Data were imported to OmniViz™ 3.6.1 (OmniViz, Maynard MA) for visualization and data mining using *Z*-score analysis. For a given protein observed within each replicate, *Z*-score was calculated by OmniViz™ as $Z_z=(x-\mu_x)/\sigma_x$, where, x is the mean abundance of peptides for a given protein, μ_x is the mean of abundances for a given protein across culture conditions and digests, and σ_x is the standard deviation associated with μ_x. This "label free" approach provided a pseudo-quantitative comparison of arbitrary abundances significant to a particular digest and growth condition and has been applied previously to proteomic studies using arbitrary abundances measured by LC-FTICR (Adkins et al., 2005).

3. Results and discussion

3.1. Global proteome analysis of R. sphaeroides 2.4.1 aerobic and photosynthetic cell cultures revealed significant protein coverage based on the current protein annotation

Approximately 6500 peptides were identified by LC-MS/MS and validated by LC-FTICR. A breakdown of these peptides by discriminant score revealed that 90% had scores of 1.0, which indicated that the peptide sequences identified by LC-MS/MS and subsequently detected by LC-FTICR measured masses and normalized elution times were of high quality (Fig. 1A). This high quality was confirmed by the decreased estimate of percent false positives in the *R. sphaeroides* PMT database observed with increased discriminant score (Fig. 1B). Although this estimate of the number of false positives applies to the LC-MS/MS portion of the AMT process, currently, a reliable and generally acceptable method of estimating percent false positives from LC-FTICR analyses is not available. However, from the number of peptides detected by LC-FTICR having high discriminant scores and from the relatively low percentage of false positives in the initial identification stage, we inferred that the percentage of false positives from the FTICR validation step was low.

These peptides matched to 1675 annotated proteins, which corresponded to ~39% coverage of predicted proteins based on JGI annotation models [http://genome.jgi-psf.org/finished_microbes/rhosp/rhosp.home.html]. Of these proteins, 1445 proteins were validated by a minimum of 2 unique peptides, corresponding to a coverage of ~34%, and viewed as very high confidence. Table 1 lists the number of proteins by genomic element. These elements for *R. sphaeroides* consist of a large chromosome (~3.2 mb) and a small chromosome (~0.9 mb) with roughly 3037 and 840 candidate proteins, respectively, and five plasmids (pRS241*a*–pRS241*e*) ranging in size from 114 kb to 37 kb with ~292 predicted proteins in total. The largest number of identified proteins (83%) was attributed to Chromosome I, which is expected considering its size relative to the

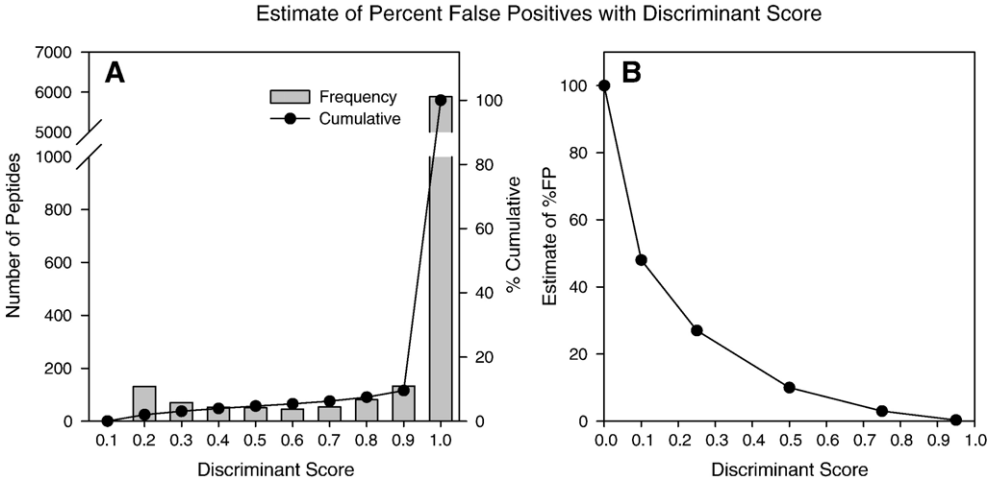

Fig. 1. A) Distribution of ~6500 peptides according to discriminant score that were identified by LC-MS/MS and subsequently detected by LC-FTICR. B) Plot of estimated percent false with increasing discriminant score for the PMT database. 90% of peptides detected by the LC-FTICR had discrimininant scores of 1.0, which inferred that the percentage of false positives from the application of the AMT approach was low.

Table 1
Identified proteins separated by genomic element

Genomic element	Predicted	Total proteome	Percent coverage	Total transcriptome	Percent coverage	Uniquely detected aerobic proteome	Uniquely detected photosynthetic proteome
Chromosome 1	3037	1197	39	2027	67	0	39
Chromosome 2	846	185	22	354	42	0	6
Plasmid a	103	21	20	50	48	0	0
Plasmid b	96	15	16	40	42	0	2
Plasmid c	79	6	8	39	49	0	1
Plasmid d	87	18	21	51	59	0	2
Plasmid e	21	3	14	13	62	0	0
Total	4269	1445	34	2574	60	0	50

Each protein was targeted by two unique peptides to add confidence to the presence of the protein within the samples. A uniquely detected protein was defined as having been observed in 6 of 9 LC-FTICR MS analyses corresponding to one condition (aerobic or photosynthetic) but not the other. For comparison, mRNAs detected in either culture condition from transcriptome data have been included.

other genomic elements. However, the number of proteins identified from plasmid d was greater than the number identified from plasmids b and c in spite of plasmid d being smaller (101 kb) than plasmids b and c (104 kb and 113 kb, respectively). Additionally, the observed percent coverage of predicted proteins for plasmid d was roughly equal to plasmid a, the largest of the five plasmids (114 kb). The larger number of proteins observed from plasmid d suggests a greater physiologic role under these two culture conditions compared to the other plasmids. This behavior was evidenced for the photosynthetic culture by two uniquely detected proteins: RSP4158 annotated as a generic methlytransferase and RSP4159 annotated as similar to a isopropyl–malate synthase or NifV-like enzymes. RSP4158 and RSP4159 reside within a small gene cluster (RSP4157–RSP4160) and are co-transcribed under photosynthetic conditions. Loss of photosynthetic activity (photoheterotrophic activity in the presence of succinate-based medium) has been observed from insertional mutation into this gene cluster, which adds additional evidence for the physiological role of this plasmid in the photosynthetic lifestyle (Tavano et al., 2005).

Open reading frames detected by mRNA transcripts from *R. sphaeroides*, cultured under the same conditions (Roh et al., 2004) are also presented in Table 1 for comparison. An ORF was considered positively identified in either culture condition by an mRNA transcript provided it was observed across all replicates and its corresponding signal intensity exceeded the background mean signal intensity by two standard deviations. Background signal intensity was measured using 24 negative control probe sets (Roh et al., 2004). Approximately 60% of predicted ORFs were detected by mRNA transcripts (http://genome.jgi-psf.org/finished_microbes/rhosp/rhosp.home.html). This percentage is significantly greater than our observed proteome coverage. We attribute the lower proteome coverage to a combination of possible factors such as, the conservative criteria used for protein identification, the masking of peptides from lower abundant proteins by peptides from proteins in higher abundance during LC separation, and possibly biological factors such as protein turnover.

In terms of the photosynthesis gene cluster (RSP0255–RSP0317) contained on Chromosome I, 32 of 62 predicted gene products were observed in at least one culture and included integral membrane proteins known to be structural components of the photosynthetic apparatus (RSP0255–RSP0259, RSP0291, RSP0314), as well as enzymes involved in carotenoid (RSP0264, RSP0271, RSP0272) and bacteriochlorophyll biosynthesis (RSP0261–RSP0263, RSP0273, RSP0274, RSP0277, RSP0279–RSP0281, RSP0285–RSP0289). Additionally, 3 peptides from the hypothetical protein RSP0295 were observed in the soluble and global protein extractions. Transcription results previously suggested this ORF plays a role in photosystem complex formation (Pappas et al., 2004).

Functional categories were assigned to predicted and identified proteins based on Clusters of Orthologous Groups (COGS) (Tatusov et al., 1997). The percentage of identified proteins compared to predicted proteins for each functional category was calculated (Fig. 2). Percentages ranged from 32% for proteins of unknown function and proteins predicted in cell division and chromosome partitioning to 75% for proteins predicted in translation and ribosomal structure (Fig. 2). For those categories in which we observed the largest coverage, many of the identified proteins were either conserved structural proteins or proteins involved in housekeeping functions.

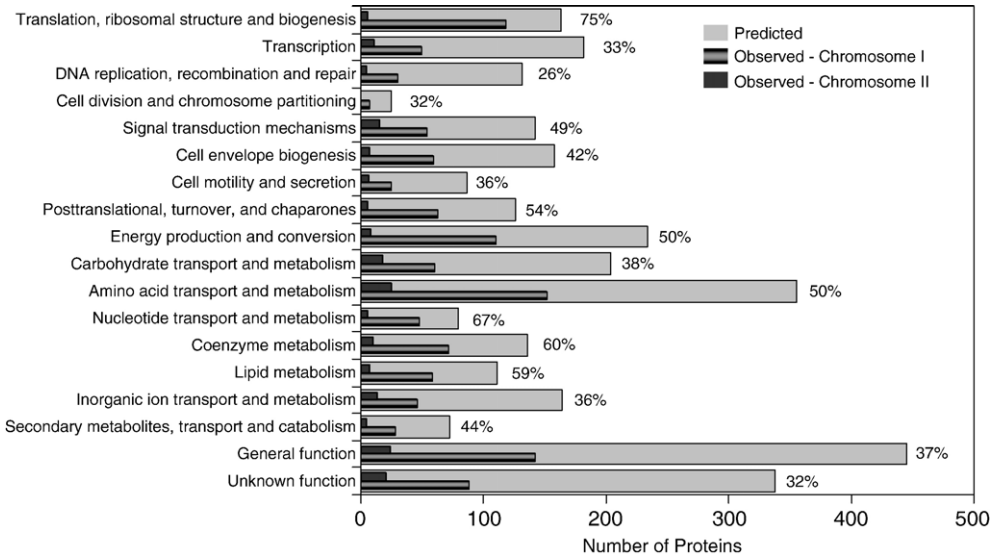

Fig. 2. Functional categories assigned to predicted and identified proteins based on clusters of orthologous groups (COGS). Percentages were calculated from the number of identified proteins compared to the number of predicted proteins for a functional category. This comparison was made for all identified proteins and these proteins grouped by chromosome.

However, of the identified proteins described as having an unknown function, 108 were described as hypothetical proteins with a majority associated with Chromosome I. Fig. 3 displays heat maps for 38 of these hypothetical proteins according to the their observation within the insoluble and soluble protein preparations. The remaining hypothetical proteins could not be placed into either one of these preparations. Based on calculated *Z*-scores, twenty of these hypothetical proteins agreed qualitatively with transcriptome measurements, in terms of a likely difference in abundance between the two cell cultures (8 — photosynthetic cell culture, 12 — aerobic cell culture). However, 12 hypothetical proteins qualitatively disagreed between proteome and transcriptome measurements (Fig. 3). A lack of correlation between mRNA measurements and proteome measurement is often observed (Gygi et al., 1999; Nie et al., 2006) and it has been suggested that the degree of correlation between these two platforms cannot be based on abundance measurements alone (Gygi et al., 1999). Five proteins lacked transcriptome data and 1 protein could not be differentiated relative to either cell culture. In general, hypothetical proteins are predicted as such due to little or no sequence homology to other sequenced organisms, and are often of low molecular weight or have little associated structural information. Because a minimum of two high quality peptides per protein were used for identfication (Fig. 3), these hypothetical proteins were considered confidently detected having a functional role relative to the growth conditions employed.

3.2. Evaluation of aerobic and photosynthetic proteomes revealed a significant number of uniquely detected proteins

Proteins observed in at least 6 of the 9 LC-FTICR analyses of one cell culture (either aerobic or photosynthetic) but not the other were defined as uniquely detected and subjected to further analysis. Comparison of uniquely detected proteins revealed differences in both the number of identified proteins and coverage based on genomic element (Table 1). For this study no uniquely detected proteins were observed in the aerobic cell culture. Of the 50 uniquely detected proteins observed in the photosynthetic cell culture, 7 proteins (RSP0262, RSP0277, RSP280, RSP0464, RSP0466, RSP1284, RSP3266) were further supported by transcriptome data (Roh et al., 2004) (Table 2), i.e., significant mRNA signal intensity in the photosynthetic culture, but absent in the aerobic cell culture (signal intensity not above background in 2 of 3 replicates). Additionally, transcripts for 9 proteins were either marginally detected (signal intensity not significantly above background) in the aerobic cell culture or their relative expression in the photosynthetic cell culture was at least 10-fold greater suggesting very low abundance in the aerobic culture. Transcripts for the majority of the remaining proteins were significantly detected in both culture conditions, but exhibited relative expression greater in the photosynthetic cell culture (Table 2). From these uniquely detected proteins, 9 were annotated as conserved hypothetical, or hypothetical,

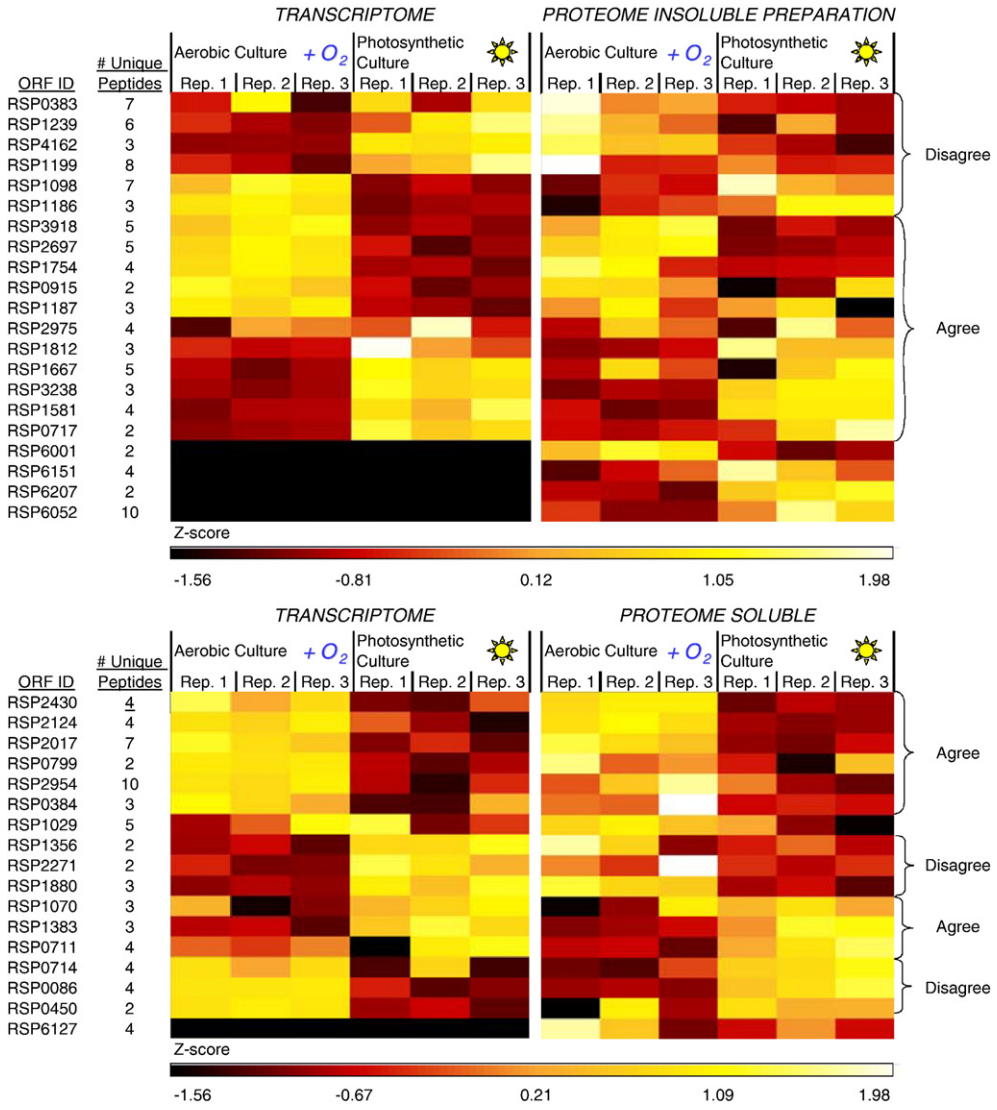

Fig. 3. Heat map comparison of calculated *Z*-scores for hypothetical proteins detected in the soluble and insoluble protein extracts. Calculated *Z*-scores are compared for data obtained from both proteome and transcriptome measurements. Proteins in qualitative agreement and disagreement with transcriptome measurements are bracketed.

(Table 2) confirming their presence as actual proteins. The presence of transcripts in both cell cultures for many of the proteins we observed as uniquely detected is possibly due to the selection of our signal to noise ratio (at least 5), where peptides from one cell culture fell below this threshold, but were above this threshold in the other cell culture. For the microarray experiments a signal intensity was detected for every probe, whether it was statistically relevant or not. A fold change threshold was set for determining the significance of a transcript present within both cell cultures (Roh et al., 2004). Additionally, transcripts for specific structural proteins involved in the photosynthetic operation of *R. sphaeroides*, have remained detectable even though rapid turnover of small amounts of these proteins have been observed under aerobic cell conditions(Varga and Kaplan, 1993). Thus, it is feasible that this occurrence can be extended to some of the proteins uniquely detected in the photosynthetic culture, but observed in both cell cultures by transcriptome measurments.

We observed with interest gene products from RSP0280 (BchJ) corresponding to Bacteriochlorophyll synthase, RSP0262 corresponding to the BchX subunit of Chlorophyllide reductase, and RSP0277 (BchP) corresponding to Geranylgeranyl bacteriochlorophyll reductase. These gene products are part of the biosynthesis pathway of

Table 2
Uniquely detected proteins within the photosynthetic cell culture

ORF identifier	Number of unique peptides	Transcriptome	Description
RSP0013	2	A	Conserved hypothetical protein
RSP0035	4	ND	Conserved hypothetical protein
RSP0069	8	PB (A>P ~3.7-fold)	Flagellar filament protein
RSP0077	5	ND	Flagellar L-ring protein
RSP0262	3	P	Chlorophyllide reductase, BchX subunit
RSP0277	4	P	Geranylgeranyl hydrogenase
RSP0280	4	P	Bacteriochlorophyll synthase
RSP0288	4	PB (P>A ~6.3-fold)	Light-independent protochlorophyllide reductase iron protein
RSP0464	5	P	Putative protease
RSP0465	5	PB (P>A ~10-fold)	Putative protease
RSP0466	2	P	Conserved hypothetical protein
RSP0762	2	PB (P>A ~1.6-fold)	Putative transcription regulator
RSP0812	3	PB (A>P ~1.4-fold)	Glyoxalase I (EC: 4.4.1.5) (lactoylglutathione lyase)
RSP1134	7	PB (P>A ~2.1-fold)	1 deoxyxylulose-5-phosphate synthase
RSP1257	4	PB (P>A ~3.7-fold)	Putative polyhydroxyalkanoic synthase
RSP1281	1	P, MA	Ribulose bisphosphate carboxylase, small subunit
RSP1282	9	P, MA	Ribulose bisphosphate carboxylase, large subunit
RSP1284	5	P	Phosphoribulokinase; putative leader peptide sequence
RSP1467	2	PB (P>A ~70-fold)	Possible alkane hydroxylase (fatty acid desaturase)
RSP1474	6	PB	Putative carboxynorspermidine decarboxylase protein
RSP1584	14	MP, A	Chemotaxis histidine protein kinase
RSP1585	2	A	Chemotaxis protein, CheW2
RSP1586	2	A	Chemotaxis protein, CheW3
RSP1621	3	PB (A>P ~2.5-fold)	Deoxyguanosinetriphosphate triphosphohydrolase-like protein
RSP1760	4	PB (P>A ~9.8-fold)	Hypothetical protein
RSP1762	4	PB (P>A ~12-fold)	Hypothetical
RSP1763	5	PB (A>P ~1.3-fold)	Phenylalanyl-tRNA synthetase alpha subunit
RSP2046	5	PB (P>A ~1.5-fold)	Hypothetical
RSP2108	2	PB (A>P ~1.7-fold)	UDP-*N*-acetylmuramate-alanine ligase
RSP2320	2	PB (P>A ~2.2-fold)	TRAP-T family transporter, periplasmic binding protein
RSP2602	2	A	ABC phosphate transporter, inner membrane subunit PstA
RSP2712	4	PB	Probable 3-hydroxymyristoyl/3-hydroxydecanoyl-(acyl carrier protein) dehydratase
RSP2768	3	P, MA	5-methyltetrahydrofolate *S*-homocysteine methyltransferase
RSP2820	2	PB (A>P ~1.3-fold)	Putative uroporphyrin-III C-methyltransferase
RSP2839	2	PB	Nitrogen regulation protein
RSP4041	4	PB (A>P ~2.4-fold)	Tyrosyl-tRNA synthetase, class Ib
RSP6023	3	ND	Carbamoyl-phosphate synthase small chain, CPSase domain
RSP6158	3	ND	Light-harvesting complex alpha subunit with extended Cterminus (periplasmic)
RSP3059	8	PB (A>P ~2.2-fold)	ABC proline/glycine betaine transporter, periplasmic substrate-binding protein
RSP3266	4	P	Fructose-1,6-bisphosphatase
RSP3269	13	PB (P>A ~20-fold)	Glyceraldehyde 3-phosphate dehydrogenase
RSP3361	5	PB (P>A ~46-fold)	Putative restriction endonuclease or methylase
RSP3641	4	PB (P>A ~2.1-fold)	Possible pfkB family carbohydrate kinase
RSP3707	4	PB (P>A ~1.9-fold)	Conserved hypothetical protein
RSP3757	5	PB (P>A ~2.8-fold)	Conserved hypothetical protein
RSP3983[b]	2	PB	Circadian clock protein KaiB homolog
RSP3986[b]	5	PB (P>A~3.8-fold)	Conserved hypothetical protein
RSP4086[c]	5	MP, A	Polysaccharide export protein
RSP4158[d]	12	PB (P>A ~22-fold)	Generic methyltransferase
RSP4159[d]	7	PB (P>A ~24-fold)	HMG-CoA lyase-like:Alpha-isopropylmalate/homocitrate synthase

A uniquely detected protein was defined as having been observed in one condition (aerobic or photosynthetic) by at least 6 of 9 LC-FTICR MS analyses and was not observed in any instrument analyses from the other condition. ND = no data/not detected, PB = present in both cell cultures, P = present in photosynthetic culture, A = present in aerobic culture, M = marginally present.
b = Plasmid b; c = Plasmid c; d = Plasmid d.

converting chlorophyll to bacteriochlorophyll (Addlesee and Hunter, 1999; Burke et al., 1993; Mcglynn and Hunter, 1993; Suzuki and Bauer, 1995) The absence of these subunits within the aerobic culture is expected since there is no detectable bacteriochlorophyll in the presence of high oxygen tension environments (Chory et al., 1984). Also expected was the lack of detection of RSP1281, RSP1282, and RSP1284 part of the *cbbI* operon (RSP1280–RSP1285) involved in carbon-dioxide fixation (Calvin–Benson–Bassham cycle). Two additional proteins, RSP3266 and RSP3269, from the second *cbb* operon (*cbbII* RSP3266–RSP3271) were also uniquely detected in this study. Under the photoheterotrophic conditions studied here, "excess" reducing power is produced from photosynthesis. In the presence of an external growth substrate, the role of the Calvin cycle in *R. sphaeroides* likely acts to balance the redox state of the cell (Tabita, 1988; Zhu and Kaplan, 1985).

R. sphaeroides exhibits photosensory cell movement in response to light stimulation (Armitage and Schmitt, 1997; Romagnoli and Armitage, 1999; Romagnoli et al., 2002). We observed three chemotaxis proteins uniquely detected in the photosynthetic culture. These proteins include, RSP1584, RSP1585, and RSP1586, which are from one (RSP1583–RSP1590) of three known chemotaxis operons and encode a chemotaxis histidine kinase (CheA family) and two cytoplasmic linker proteins (CheW family), respectively. The uniquely detected presence of CheA2 (RSP1584), CheW2 (RSP1585), and CheW3 (RSP1586) in at least 6 of the 9 LC-FTICR analyses from the photosynthetic culture (absent from any of the analyses from the aerobic cell cultures) was surprising because reportedly these proteins are necessary for taxis under both aerobic and photosynthetic conditions (Martin et al., 2003, 2001). Interestingly, microarray data (Roh et al., 2004) revealed that transcripts for RSP1585 and RSP1586 were detected in the aerobic cell culture, but were absent in the photosynthetic culture; contrary to our proteomic observations. Transcripts for CheA2 were marginally detected (present in one replicate, absent in the second replicate, and on the borderline of detection in the third replicate) in the photosynthetic culture, but detected with significant signal intensity in the aerobic cell culture; also contrary to our proteomic observation.

For this analysis, it is also possible that these proteins were present in the aerobic cell culture but were not detected due to: 1) modifications of their identifying peptides, i.e. phophorylation in the case of CheA with CheW interacting with the signaling domains of CheA and MCPs (methyl-accepting proteins) (Wadhams and Armitage, 2004), 2) identifying peptides that were detected but filtered out due to the selection of threshold criteria, and/or 3) proteins present below the limit of detection as a result of low copy numbers in the aerobic cell culture condition. In terms of modified peptides, the applied AMT approach does not identify these post-translational modifications, and we are currently adapting to more effectively identify potentially modified peptides. In terms of filtering thresholds, we observed a few peptides in the aerobic cell culture targeting these proteins that did not fall within our set threshold criteria. Although discriminant scores for these peptides were relatively large (0.84–1.0), their spatially localized confidence scores were relatively low (0.12–0.57, with 0.99 as the maximum possible) suggesting that the measured masses and normalized elution times were incorrectly assigned to the given peptides.

3.3. Aerobic respiration and photosynthesis require different pathways of energy generation and we evaluated the relative abundance of proteins involved in these pathways

Proteins common to both the aerobic and photosynthetic cell cultures were analyzed using *Z*-score statistics as a means of comparing significant differences in relative abundance (Adkins et al., 2005). Additionally, *Z*-score analysis provided a rough estimate of primary localization for those proteins that were identified in both the insoluble and soluble sample preparations taken from both cell cultures. For this comparison of protein abundance, we focused on bioenergetic pathways that have been characterized to varying extents biochemically, genetically, or monitored using transcriptome data (Pappas et al., 2004). We also focused on gene products annotated as hypothetical, which make up roughly 20% of the *R. sphaeroides* 2.4.1 genome.

In *R. sphaeroides*, the first step in charge separation under aerobic respiration occurs via reduction of the quinone–quinol pool via either of two NADH-ubiquinone dehydrogenases. We detected peptides that targeted the C (RSP2514), D (RSP2515), E (RSP2516), and G (RSP2521) subunits, as well as peptides derived from the iron sulfur protein complex (RSP2523, Complex 1) that makes up one of the NADH-ubiquinone dehydrogenases (RSP2512–RSP2531). No peptides were detected that targeted the second putative NADH-ubiquinone dehydrogenase (RSP0100–RSP0112). *Z*-score analysis indicated decreased relative abundance for all subunits noted above when the photosynthetic culture was compared to the aerobic culture (Fig. 4). This observation was consistent with peptides found in either the soluble or insoluble protein extractions, i.e., subunits C and D were primarily detected in the soluble fraction, which

suggests peripheral subunits, while subunits E, G, and the 2Fe–S containing subunit were detected primarily in the insoluble fraction. Our *Z*-score results were consistent, at least qualitatively, with transcriptome data, which showed 35%–60% down regulation in cognate mRNAs under anoxic conditions (Pappas et al., 2004).

We additionally identified peptides derived from the flavoprotein subunit and the iron sulfur protein complex from succinate dehydrogenase (RSP0974–RSP0979). This dehydrogenase is involved in respiration when succinate is present in the growth medium, via electron transfer to the quinone–quinol pool. Although arbitrary raw abundances for these subunits within the photosynthetic culture appeared somewhat less than in the aerobic culture, the *Z*-score analysis did not indicate a significant change in the relative abundance of either subunit. Transcriptome data for this dehydrogenase are also consistent with proteome observations (Pappas et al., 2004; Roh et al., 2004), which suggests that the succinate present in the Sistrom's growth medium is being utilized by *R. sphaeroides* as a source of carbon and reducing power in the photosynthetic cell culture in addition to carbon obtained through CO_2 fixation.

Charge separation occurs under photosynthetic conditions following energy transfer from the light harvesting complexes to the reaction center, and subsequent electron transport through the quinone–quinol pool to the cytochrome bc_1 complex. The reaction center complex is returned to its ground redox state via reduction by cytochrome bc_2. We observed peptides for the PufM, PufL, and PufH subunits (RSP0256, RSP0257, RSP0291) of the reaction center, which exhibited significant differentiation in *Z*-score (Fig. 4) between the photosynthetic and aerobic cell cultures, indicating a large increase in the relative

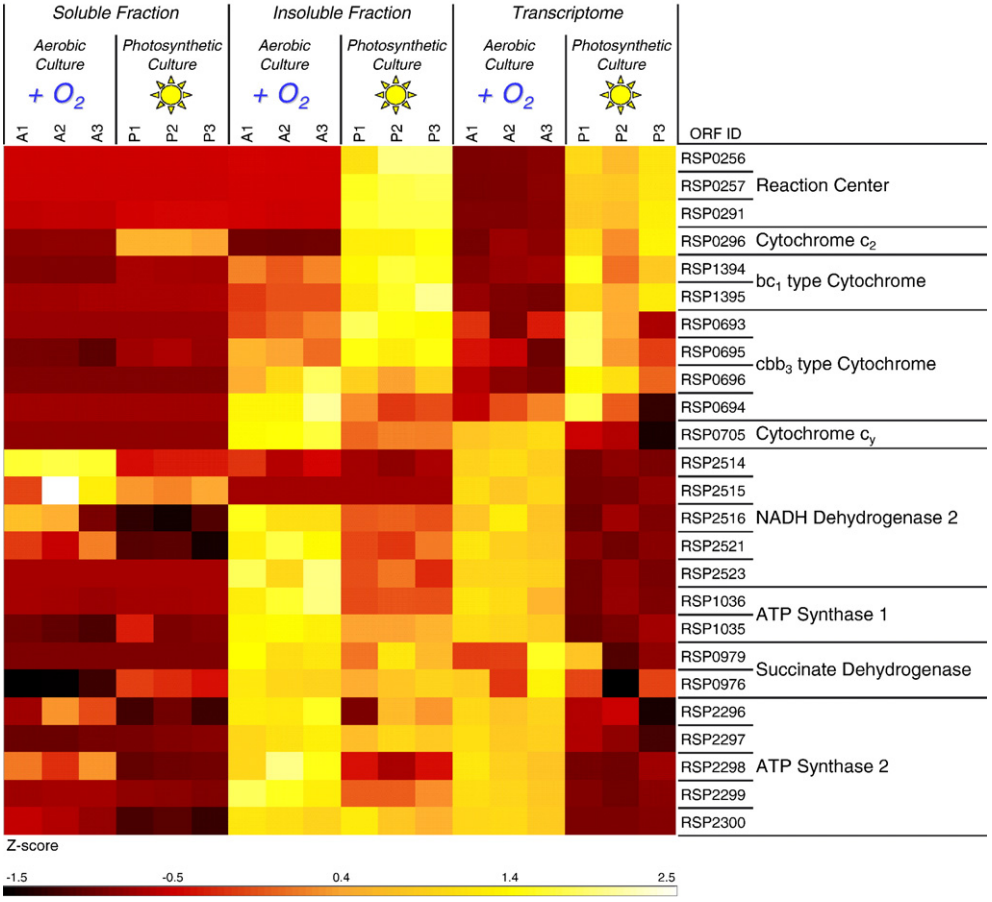

Fig. 4. Heat map comparisons of *Z*-scores between proteins involved in electron transfer detected in either or both the soluble and insoluble sample preparations. Increasing intensity in the positive range represents abundances that are greater than the mean abundance derived from both culture conditions and sample preparations relative to the standard deviation associated with the mean. Decreasing intensity in the negative range represents abundances that are less than the mean abundance relative the standard deviation. A majority of proteins showed a greater affinity for the insoluble preparation. *Z*-score values for the aerobic and photosynthetic cell cultures also suggest the growth condition in which the protein was observed with the greatest abundance.

abundance of these subunits. Peptides for 2 subunits of the cytochrome bc_1 complex, cytochrome c_1 (RSP1394) and cytochrome b (RSP1395), were also observed to significantly increase in relative abundance, which indicates an additional requirement of this complex in relation to the photosystem complex.

Peptides for both cytochromes c_2 and c_y (RSP0296, RSP0705) were observed to behave inversely, i.e., the Z-score for cytochrome c_2 indicated an increase in relative abundance for the photosynthetic culture while the Z-score for cytochrome c_y indicated a decrease in relative abundance (Fig. 4). The down regulation and up regulation of these cytochromes has been observed from the transcriptome data as well (Pappas et al., 2004). Our proteome observations for these soluble cytochromes are also consistent with previous studies that demonstrated the requirement of cytochrome c_2 for photosynthetic growth, but that cytochrome c_y is not required for photosynthetic growth (Daldal et al., 2001; Donohue et al., 1988). These cytochromes are responsible for passing electrons to two respiratory oxidases, cbb_3 and aa_3, over a wide range of oxygen tensions (Dmello et al., 1996; Preisig et al., 1996). From the cbb_3 type cytochrome oxidase, peptides that target the CcoN (RSP0696), O (RSP0695), P (RSP0693) and Q (RSP0694) subunits were detected in both cell cultures. CcoO and CcoP showed increased relative abundances in the photosynthetic cell culture ($\sim 1.7 \pm 0.3$ for CcoO, $\sim 2.8 \pm 0.8$ for CcoP), while the Z-score for the CcoN subunit indicated neither a significant increase nor decrease in relative abundance in the photosynthetic cell culture ($\sim 1.1 \pm 0.3$). CcoQ exhibited increased relative abundance in the aerobic cell culture ($\sim 2.8 \pm 0.1$). Reasons for the disparity among the relative abundances of subunits that make up this terminal oxidase are unclear. However, transcriptome data reported for this oxidase indicated a slight increase in relative abundance in the photosynthetic cell culture, ranging from 1.15 to 2-fold (Pappas et al., 2004).

Three ATP synthases are predicted from the genome sequence of *R. sphaeroides*, 2 encoded on Chromosome I and the remaining encoded on plasmid a. Both chromosomal encoded ATP synthases were observed in this study (Fig. 4). For the upstream encoded ATP synthase, peptides corresponding to ORFs RSP1036 and RSP1035, both annotated as subunit B, were detected. Z-score analysis suggested a difference in abundance between the aerobic and photosynthetic cell cultures with the relative abundances greater in the aerobic cell culture compared to the photosynthetic cell culture. For the downstream ATP synthase, peptides corresponding to 5 ORFs (RSP2296–RSP2300) were detected. With the exception of the γ and β subunits (RSP2298 and RSP2299), it was difficult to distinguish whether measured abundances for the remaining subunits were different on the basis of their Z-scores. For the γ and β subunits, an increased relative abundance in the aerobic cell culture was suggested. Transcriptome data for RSP1035, RSP1036, RSP2298, and RSP2299 supported proteome observations for these subunits (Roh et al., 2004). However, these ATP synthases, in whole, reportedly do not change in relative abundance between oxic and anoxic-light conditions (Pappas et al., 2004).

4. Conclusions

Our results highlighted proteins directly or indirectly associated with the photosynthetic lifestyle of *R. sphaeroides* in addition to those proteins originating from the photosynthetic gene complex. Additionally, transcriptome measurements provided a complimentary measure of gene expression, as demonstrated by the identification and comparison of proteins involved in chemotaxis, sensory, and electron transport. Although in some instances transcriptome and proteome data were in apparent conflict, the meaning and significance of these instances remains uncertain, but not unexpected (Nie et al., 2006) possibly from experimental challenges, and from biological processes such as RNA and protein turnover. Nevertheless, the high-throughput nature of the proteome data obtained using LC-MS methods and the AMT tag approach allowed a diverse set of soluble and membrane bound proteins to be identified, aiding the further establishment and connection of models of photosynthetic behavior. A greater understanding of this photosynthetic behavior is and will be important to applying the unique abilities of *R. sphaeroides*. For example, the rate of hydrogen production by *R. sphaeroides* is related to the amount of light intensity (Miyake and Kawamura, 1987) which is inversely related to the number of light harvesting complexes (B800-850-LHII). This study provides a baseline for future large scale proteomic studies utilizing our high-throughput proteomic approach.

Acknowledgements

Portions of this work were supported by the U.S. Department of Energy (DOE) Office of Biological and Environmental Research, grant (ER63232-1018220-0007203), and United States Public Health Service grant (USPHS GM15590). Experimental portions of this research were performed in the Environmental Molecular Sciences Laboratory, a DOE national scientific user facility located at Pacific Northwest National Laboratory in Richland, Washington. We thank J.N. Adkins and N.

G. Colton for critical and editorial reviews of this work, and N. Toliæ and M.E. Monroe for development of the data analysis tools. Pacific Northwest National Laboratory is a multiprogram national laboratory operated by Battelle for the DOE under Contract DE-AC05-76RL01830.

References

Addlesee, H.A., Hunter, C.N., 1999. Physical mapping and functional assignment of the geranylgeranyl-bacteriochlorophyll reductase gene, *bchP*, of *Rhodobacter sphaeroides*. J. Bacteriol. 181, 7248–7255.

Adkins, J.N., Monroe, M.E., Auberry, K.J., Shen, Y.F., Jacobs, J.M., Camp, D.G., Vitzthum, F., Rodland, K.D., Zangar, R.C., Smith, R.D., Pounds, J.G., 2005. A proteomic study of the HUPO Plasma Proteome Project's pilot samples using an accurate mass and time tag strategy. Proteomics 5, 3454–3466.

Anderson, K.K., Monroe, M.E., Daly, D.S., 2004. Estimating probabilities of peptide assignments to LC-FTICR-MS observations. Proc of the Intern Conf METMBS, pp. 151–156.

Armitage, J.P., Schmitt, R., 1997. Bacterial chemotaxis: *Rhodobacter sphaeroide*s and *Sinorhizobium meliloti* — variations on a theme? Microbiology 143, 3671–3682.

Belov, M.E., Anderson, G.A., Wingerd, M.A., Udseth, H.R., Tang, K.Q., Prior, D.C., Swanson, K.R., Buschbach, M.A., Strittmatter, E.F., Moore, R.J., Smith, R.D., 2004. An automated high performance capillary liquid chromatography-Fourier transform ion cyclotron resonance mass spectrometer for high-throughput proteomics. J. Am. Soc. Mass Spectrom. 15, 212–232.

Bolstad, B.M., Irizarry, R.A., Astrand, M., Speed, T.P., 2003. A comparison of normalization methods for high density oligonucleotide array data based on variance and bias. Bioinformatics 19, 185–193.

Burke, D.H., Alberti, M., Hearst, J.E., 1993. The *Rhodobacter capsulatus* chlorin reductase-encoding locus, *bchA*, consists of 3 genes, *bchX*, *bchy*, and *bchZ*. J. Bacteriol. 175, 2407–2413.

Chory, J., Donohue, T.J., Varga, A.R., Staehelin, L.A., Kaplan, S., 1984. Induction of the photosynthetic membranes of *Rhodopseudomonas sphaeroides* — biochemical and morphological studies. J. Bacteriol. 159, 540–554.

Choudhary, M., Kaplan, S., 2000. DNA sequence analysis of the photosynthesis region of *Rhodobacter sphaeroides* 2.4.1. Nucleic Acids Res. 28, 862–867.

Cohen-Bazire, G., Sistrom, W.R., Stanier, R.Y., 1957. Kinetic studies of pigment synthesis by non-sulfur purple bacteria. J. Cell. Comp. Physiol. 49, 25–68.

Daldal, F., Mandaci, S., Winterstein, C., Myllykallio, H., Duyck, K., Zannoni, D., 2001. Mobile cytochrome c_2 and membrane-anchored cytochrome *cy* are both efficient electron donors to the cbb_3- and aa_3-type cytochrome *c* oxidases during respiratory growth of *Rhodobacter sphaeroides*. J. Bacteriol. 183, 2013–2024.

Dmello, R., Hill, S., Poole, R.K., 1996. The cytochrome *bd* quinol oxidase in *Escherichia coli* has an extremely high oxygen affinity and two oxygen-binding haems: implications for regulation of activity in vivo by oxygen inhibition. Microbiology-Uk 142, 755–763.

Donohue, T.J., Mcewan, A.G., Vandoren, S., Crofts, A.R., Kaplan, S., 1988. Phenotypic and genetic characterization of cytochrome c_2 deficient mutants of *Rhodobacter sphaeroides*. Biochemistry 27, 1918–1925.

Dubbs, J.M., Tabita, F.R., 2004. Regulators of nonsulfur purple phototrophic bacteria and the interactive control of CO_2 assimilation, nitrogen fixation, hydrogen metabolism and energy generation. FEMS Microbiol. Rev. 28, 353–376.

Eng, J.K., Mccormack, A.L., Yates, J.R., 1994. An approach to correlate tandem mass-spectral data of peptides with amino-acid-sequences in a protein database. J. Am. Soc. Mass Spectrom. 5, 976–989.

Fang, H.H.P., Liu, H., Zhang, T., 2005. Phototrophic hydrogen production from acetate and butyrate in wastewater. Int. J. Hydrogen Energy 30, 785–793.

Gygi, S.P., Rochon, Y., Franza, B.R., Aebersold, R., 1999. Correlation between protein and mRNA abundance in yeast. Mol. Cell. Biol. 19, 1720–1730.

Joshi, H.M., Tabita, F.R., 1996. A global two component signal transduction system that integrates the control of photosynthesis, carbon dioxide assimilation, and nitrogen fixation. Proc. Natl. Acad. Sci. U. S. A. 93, 14515–14520.

Lipton, M.S., Pasa-Tolic, L., Anderson, G.A., Anderson, D.J., Auberry, D.L., Battista, K.R., Daly, M.J., Fredrickson, J., Hixson, K.K., Kostandarithes, H., Masselon, C., Markillie, L.M., Moore, R.J., Romine, M.F., Shen, Y.F., Stritmatter, E., Tolic, N., Udseth, H.R., Venkateswaran, A., Wong, L.K., Zhao, R., Smith, R.D., 2002. Global analysis of the *Deinococcus radiodurans* proteome by using accurate mass tags. Proc. Natl. Acad. Sci. U. S. A. 99, 11049–11054.

Martin, A.C., Wadhams, G.H., Armitage, J.P., 2001. The roles of the multiple CheW and CheA homologues in chemotaxis and in chemoreceptor localization in *Rhodobacter sphaeroides*. Mol. Microbiol. 40, 1261–1272.

Martin, A.C., Nair, U., Armitage, J.P., Maddock, J.R., 2003. Polar localization of $CheA_2$ in *Rhodobacter sphaeroides* requires specific Che homologs. J. Bacteriol. 185, 4667–4671.

Martinezluque, M., Dobao, M.M., Castillo, F., 1991. Characterization of the assimilatory and dissimilatory nitrate-reducing systems in *Rhodobacter* — a comparative study. FEMS Microbiol. Lett. 83, 329–334.

Mcglynn, P., Hunter, C.N., 1993. Genetic analysis of the *bchC* gene and *bchA* gene of *Rhodobacter sphaeroides*. Mol. Gen. Genet. 236, 227–234.

Miyake, J., Kawamura, S., 1987. Efficiency of light energy conversion to hydrogen by the photosynthetic bacterium *Rhodobacter sphaeroides*. Int. J. Hydrogen Energy 12, 147–149.

Moore, M.D., Kaplan, S., 1992. Identification of intrinsic high-level resistance to rareearth-oxides and oxyanions in members of the class proteobacteria – characterization of tellurite, selenite, and rhodium sesquioxide reduction in *Rhodobacter sphaeroides*. J. Bacteriol. 174, 1505–1514.

Nepple, B.B., Kessi, J., Bachofen, R., 2000. Chromate reduction by *Rhodobactor sphaeroides*. J. Ind. Microbiol. Biotech. 25, 198–203.

Nie, L., Wu, G., Zhang, W.W., 2006. Correlation between mRNA and protein abundance in *Desulfovibrio vulgaris*: a multiple regression to identify sources of variations. Biochem. Biophys. Res. Commun. 339, 603–610.

Norbeck, A.D., Monroe, M.E., Adkins, J.N., Anderson, K.K., Daly, D.S., Smith, R.D., 2005. The utility of accurate mass and LC elution time information in the analysis of complex proteomes. J. Am. Soc. Mass Spectrom. 16, 1239–1249.

Pappas, C.T., Sram, J., Moskvin, O.V., Ivanov, P.S., Mackenzie, R.C., Choudhary, M., Land, M.L., Larimer, F.W., Kaplan, S., Gomelsky, M., 2004. Construction and validation of the *Rhodobacter sphaeroides* 2.4.1 DNA microarray: transcriptome flexibility at diverse growth modes. J. Bacteriol. 186, 4748–4758.

Preisig, O., Zufferey, R., Thonymeyer, L., Appleby, C.A., Hennecke, H., 1996. A high-affinity cbb3-type cytochrome oxidase terminates the

symbiosis-specific respiratory chain of *Bradyrhizobium japonicum*. J. Bacteriol. 178, 1532–1538.

Qian, W.J., Liu, T., Monroe, M.E., Strittmatter, E.F., Jacobs, J.M., Kangas, L.J., Petritis, K., Camp, D.G., Smith, R.D., 2005. Probability-based evaluation of peptide and protein identifications from tandem mass spectrometry and SEQUEST analysis: the human proteome. J. Proteome Res. 4, 53–62.

Roh, J.H., Smith, W.E., Kaplan, S., 2004. Effects of oxygen and light intensity on transcriptome expression in *Rhodobacter sphaeroides* 2.4.1: redox active gene expression profile. J. Biol. Chem. 279, 9146–9155.

Romagnoli, S., Armitage, J.P., 1999. Roles of chemosensory pathways in transient changes in swimming speed of *Rhodobacter sphaeroides* induced by changes in photosynthetic electron transport. J. Bacteriol. 181, 34–39.

Romagnoli, S., Packer, H.L., Armitage, J.P., 2002. Tactic responses to oxygen in the phototrophic bacterium *Rhodobacter sphaeroides* WS8N. J. Bacteriol. 184, 5590–5598.

Schultz, J.E., Weaver, P.F., 1982. Fermentation and anaerobic respiration by Rhodospirillum rubrum and Rhodopseudomonas capsulata. J. Bacteriol. 149, 181–190.

Smith, R.D., Anderson, G.A., Lipton, M.S., Pasa-Tolic, L., Shen, Y.F., Conrads, T.P., Veenstra, T.D., Udseth, H.R., 2002. An accurate mass tag strategy for quantitative and high-throughput proteome measurements. Proteomics 2, 513–523.

Strittmatter, E.F., Kangas, L.J., Petritis, K., Mottaz, H.M., Anderson, G.A., Shen, Y.F., Jacobs, J.M., Camp, D.G., Smith, R.D., 2004. Application of peptide LC retention time information in a discriminant function for peptide identification by tandem mass spectrometry. J. Proteome Res. 3, 760–769.

Suzuki, J.Y., Bauer, C.E., 1995. Altered monovinyl and divinyl protochlorophyllide pools in *bchJ* mutants of *Rhodobacter capsulatus*. J. Biol. Chem. 270, 3732–3740.

Tabita, F.R., 1988. Molecular and cellular regulation of autotrophic carbon dioxide fixation in microorganisms. Microbiol. Rev. 52, 155–189.

Tatusov, R.L., Koonin, E.V., Lipman, D.J., 1997. A genomic perspective on protein families. Science 278, 631–637.

Tavano, C.L., Podevels, A.M., Donohue, T.J., 2005. Identification of genes required for recycling reducing power during photosynthetic growth. J. Bacteriol. 187, 5249–5258.

Varga, A.R., Kaplan, S., 1993. Synthesis and stability of reaction center polypeptides and implications for reaction center assembly in *Rhodobacter sphaeroides*. J. Biol. Chem. 268, 19842–19850.

Wadhams, G.H., Armitage, J.P., 2004. Making sense of it all: bacterial chemotaxis. Nat. Rev. 5, 1024–1037.

Woese, C.R., 1987. Bacterial evolution. Microbiol. Rev. 51, 221–271.

Woese, C.R., Weisburg, W.G., Paster, B.J., Hahn, C.M., Tanner, R.S., Krieg, N.R., Koops, H.P., Harms, H., Stackebrandt, E., 1984. The phylogeny of purple bacteria: the beta-subdivision. Syst. Appl. Microbiol. 5, 327–336.

Yen, H.C., Marrs, B., 1977. Growth of *Rhodopseudomonas capsulata* under anaerobic dark conditions with dimethyl-sulfoxide. Arch. Biochem. Biophys. 181, 411–418.

Zeilstra-Ryalls, J., Gomelsky, M., Eraso, J.M., Yeliseev, A., O'gara, J., Kaplan, S., 1998. Control of photosystem formation in *Rhodobacter sphaeroides*. J. Bacteriol. 180, 2801–2809.

Zhu, Y.S., Kaplan, S., 1985. Effects of light, oxygen, and substrates on steady-state levels of mRNA coding for ribulose-1,5-bisphosphate carboxylase and light-harvesting and reaction center polypeptides in *Rhodopseudomonas sphaeroides*. J. Bacteriol. 162, 925–932.